Effect of convection and B_1 inhomogeneity on singlet relaxation experiments

B. Kharkov, X. Duan, J. W. Canary, and A. Jerschow*

Department of Chemistry, New York University, 100 Washington Sq. East, New York, NY 10003 USA
E-mail: alexej.jerschow@nyu.edu

Abstract

Nuclear spin singlet lifetimes can often exceed the T_1 length scales by a large factor. This property makes them suitable for polarization storage. The measurement of such long lifetimes itself can become challenging due to the influence of even very weak relaxation mechanisms. Here we show that a judicious choice of the singlet-to-triplet conversion method is highly important in order to achieve reliable singlet relaxation measurements. In particular, we identify thermal convection, in connection with B_1 field gradients, as a significant apparent decay mechanism, which limits the ability to measure the true singlet state lifetimes. Highly B_1-compensated broadband singlet excitation/detection sequences are shown to minimize the influence of macroscopic molecular motion and B_1 inhomogeneity.

Research highlights

- The effect of convection and B_1 inhomogeneity on singlet lifetime measurements is shown;
- A thermal convection model is shown to explain the experimental results;
- Sample spinning can alleviate convection artifacts, but also sample confinement, and highly inhomogeneity-compensated pulses. ;

Keywords

Convection, singlet order, singlet relaxation, SLIC, M2S, composite pulses.

1. Introduction

Two spin-1/2 nuclei of the same kind close to magnetic equivalence can form sustainable spin-zero singlet states that are immune to the main source of NMR relaxation, the intra-pair dipole-dipole coupling [1-8]. With suitable symmetry, further relaxation mechanisms may be suppressed [9]. For these reasons, singlet order may have a very long lifetime that can sometimes be significantly larger than conventional longitudinal relaxation T_1 constants. For example, lifetimes as long as 26 min and 1 hr were obtained for ^{15}N and ^{13}C singlets, respectively [10, 11]. A number of experimental techniques have been developed for singlet-to-triplet conversion. Continuous irradiation based Spin-Lock Induced Crossing (SLIC) [12-16], and J-coupling synchronized 180-degrees pulse trains (M2S) [17, 18], have been demonstrated to be efficient for generating and detecting singlet order in highly symmetric two- and homonuclear four-spin systems. Other methods, such as phase cycling in combination with rf irradiation were used for studying relaxation of singlets far from magnetic equivalence [1, 19, 20]. Due to the potentially long lifetimes, singlet states have been suggested for imaging [21], studying slow diffusion and transport processes [22-24], detecting slow flow and diffusion [25], measuring molecular parameters [26, 27], studying protein folding [28], and for extending polarization lifetimes in hyperpolarization experiments [15, 29]. In recent years, significant progress has been achieved in studying singlet relaxation mechanisms [16, 30], but the lifetime limiting mechanisms are not fully understood yet. Further insights into the pathways of singlet relaxation are desired, which requires the ability to measure very slow relaxation processes (on the order of hundreds of seconds to hours) with high accuracy.

In singlet lifetime measurements with SLIC and M2S, we have noticed strong deviations from the expected lifetimes, and we have identified collective motion in combination with B_1 inhomogeneities as the culprit for the problem. The effect is based on a spatial non-uniformity in singlet-to-triplet conversions, which, coupled with fluid motion during the long relaxation delays, leads to time-dependent signal losses, which could be mistaken as singlet relaxation processes.

It is well known that collective motional patterns such as circular convection flows may occur in an NMR tube in the presence of temperature gradients [31-35]. Convection has been demonstrated to affect, for example, the measured T_1 constants for ^{129}Xe and ^{19}F in xenon gas and xenon difluoride dissolved in deuterated cyclohexane and acetonitrile. In that experiment, convection manifested itself in the apparent reduction of T_1 constants and nonexponential, sometimes oscillatory, behavior of longitudinal magnetization decays. In the case of T_1, the effect was explained by the displacement of the molecules affected by the rf pulse sequence by

those that initially were located outside of the effective coil region. It was shown that sample spinning could help to suppress motion [36]. Similarly, it was shown that DNP-hyperpolarized spin injection, as a result of motion could lead to the appearance of multiple signal bursts, although thermal convection was not specifically described as the underlying mechanism [37].

Here we show that singlet relaxation experiments are complicated by macroscopic molecular motion during the singlet storage period. Moreover, since the lifetimes of singlet order can sometimes exceed hundreds of seconds, this type of experiment is particularly susceptible to even very slow fluid flow, which would be undetectable otherwise. We wish to point out that the type of thermal convection motion that is considered here appears to be caused due to the small temperature gradients present even without sample heating in room temperature probes [38]. Such effects can be assumed to be particularly strong for cryoprobes where temperature gradients arise from the proximity of the low-temperature tuned circuit.

In the present work, our aim was to study the effect of convection on the apparent singlet relaxation constants and investigate experimental measures that allow eliminating undesirable effects. We demonstrate that convection significantly influences the singlet relaxation measurement under standard experimental conditions and compare the performance of two most widely used singlet generation approaches, SLIC and M2S. Furthermore, we describe the ability of low-frequency sample spinning and mismatch compensated experimental rf sequences to eliminate or significantly suppress convection artifacts. Diffusion is typically too slow to have an effect such as the one due to convection, since the mean displacement is much smaller than the length scale of B_1 field changes. Nevertheless, the solution that we suggest for eliminating convection will be valid for any type of molecular displacement which includes diffusion. These results indicate that accurate singlet lifetime measurements require the specific consideration of the effects of convection, in particular due to the typically long delays needed in these experiments.

2. Theory and convection model

Convection occurs as a result of local vertical and horizontal temperature gradients, and consequently density gradients in liquid samples. Ostroumov has provided a criterion for the onset of convection in a long cylinder of radius R [39], as given by the critical Rayleigh number:

$$Ra = \frac{g\beta\rho^2 c_p}{\eta\kappa} R^4 \frac{dT}{dz}, \quad (1)$$

where g is the acceleration due to gravity, β is the thermal expansion coefficient, ρ is the fluid density of sample, c_p is the specific heat capacity, dT is the temperature difference over a dz

height, η is the dynamic viscosity and κ is the thermal conductivity. When the Rayleigh number for the system exceeds 67.4 and 215.8 for insulating and perfectly conducting media, respectively, the liquid loses its stability and sustainable circular flows occur in the sample. The theoretical equation for the velocity distribution in a long cylinder is given as the solution of the Navier-Stokes equation and takes the form [39, 40]:

$$v(r,\phi) = \sum_n v_n \cos(n\phi)\left(\frac{I_n(kr)}{I_n(kR)} - \frac{J_n(kr)}{J_n(kR)}\right), \qquad k^4 = Ra, \tag{2}$$

where J_n and I_n are the Bessel and modified Bessel functions of the first kind, respectively, v_n are system-dependent constants that decrease strongly with increasing n and are zero for even n.

As can be seen from Eq. 1 the critical Rayleigh number depends on the viscosity of the liquid, shape of the vessel, and temperature gradients over the sample dimensions. In the described model, only the vertical gradient is taken into account and the sample is assumed to be long compared to its radius. In practice, horizontal components of the temperature gradients are always present, which facilitates the onset of convection and leads to deviations from theory [41]. Furthermore, several circular flow patterns and some mixing may occur. Figure 1 shows the vertical velocity profile according to Eq. 2 corresponding to the principal antisymmetric mode $n = 1$, across an NMR tube for chloroform at 300K in the presence of a vertical temperature gradient of 1.65 K/cm. The corresponding velocity spectrum is shown in Figure 1b. This distribution was used for the fitting of the experimental decays for the SLIC experiments in long samples and has proved to provide an excellent fit without further adjustable parameters.

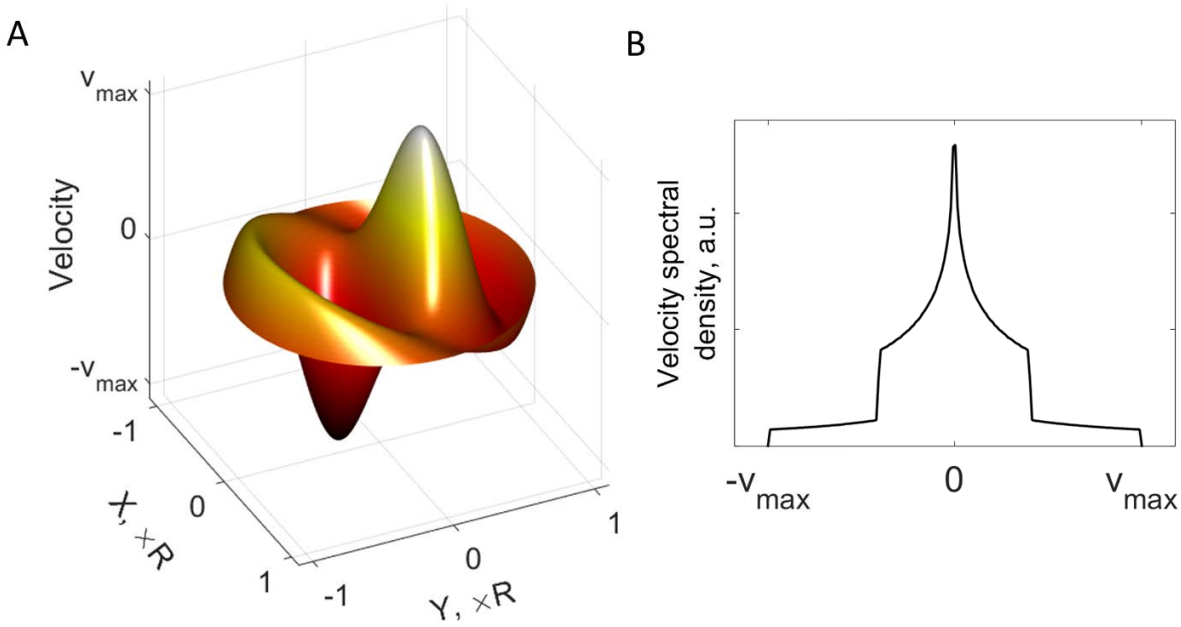

Fig. 1. (A) Spatial dependence of vertical convective flow velocity corresponding to the main mode $n = 1$ of Eq. (2) and $Ra = 1400$, calculated for a chloroform sample in a 5 mm NMR tube and (B) corresponding vertical velocity distribution.

Organic solvents, such as chloroform, acetone, methanol and others are particularly prone to heat convection, mainly because of their low viscosities and high thermal expansion coefficients. Several intuitive ways to overcome convection include using narrower NMR tubes, inserting capillaries in the tube, reducing temperature gradients, or using solvents with higher viscosity and lower thermal expansion coefficients. The first three are associated with considerable experimental complications, especially when sample degassing is needed, while the latter can be undesirable due to the specifics of the problem under study. Another possible approach is sample spinning which causes shifting of the direction of the gravitational acceleration due to the centripetal acceleration. It was demonstrated that even low speed sample spinning was highly effective for suppressing convection artifacts in T_1 relaxation measurements [36].

Convection itself cannot affect the spin dynamics and relaxation of the system provided that the molecular transport occurs between regions with the same experimental conditions, for example with the same rf field efficiency. In the case of the singlet relaxation measurement, convection interferes with the spatial nonuniformity of singlet/triplet conversion efficiency. In the extreme case, the generated singlets can leave the active coil region due to convection, thus causing additional apparent attenuation of the detected singlet signal. One can easily confine the sample within the active coil region, but, as demonstrated below, the nonuniformity of the conversion efficiency driven by B_1 inhomogeneity can also lead to significant motional artifacts.

3. Experimental

All reagents were purchased from commercial sources and used without further purification. Maleic anhydride and ethanol-d_6 anhydrous, were purchased from Sigma Aldrich. n-propyl-d_7 alcohol was purchased from C/D/D isotope. Dimethyl maleate (DMM) and triethylamine were purchased from Fisher Scientific. All NMR solvents were purchased from Cambridge Isotopes. All compounds were analyzed by Bruker AV-400 (400 MHz), AV-500 (500 MHz) and AVIII-600 (600 MHz). Deuterated asymmetric maleate acid esters were synthesized from maleic anhydride by following the procedure in the literature [42]. All reactions sensitive to moisture were done under inert atmosphere (Ar protection) with use of anhydrous solvents taken from standard solvent-drying system. Constricted sealable NMR tubes were purchased from Norell. All sample solutions were made under vacuum with freeze-pump-

thaw degassing and flame-sealing techniques. The height of the solution in an NMR tube was 9 mm. The height of a concentrated DMM solution in deuterated methanol for the SLIC imaging experiment was 33 mm.

Singlet and T_1 relaxation experiments were performed at magnetic fields of 11.74 T and 14.1 T on Bruker AV-500 (500 MHz) and AVIII-600 (600 MHz), equipped with a standard solution state triple resonance BBO probe, and a triple resonance cryoprobe, respectively. The sample temperature was controlled at 298 K. Longitudinal relaxation times (T_1) were measured using the standard saturation recovery technique. The radio frequency field strength in the T_1 and M2S experiments [17, 18] was $\gamma B_1/2\pi = 13.9$ kHz at 500 MHz and $\gamma B_1/2\pi = 31.3$ kHz at 600 MHz. The spin lock power in the SLIC experiment was 12 Hz. The echo number parameters in M2S were $n_1 = 18$ (500 MHz) and $n_1 = 14$ (600 MHz), $n_2 = n_1/2$ and the echo delay was $\tau = 20.6$ ms, which corresponded to an in-singlet *J*-coupling constatnt $J = 12$ Hz and the intra-singlet chemical shift difference was $\Delta\delta = 2.2 * 10^{-3}$ ppm. The refocusing elements were cycled according to the MLEV4 (0, 0, 2, 2) scheme [43]. The *z*-gradient field applied in the imaging experiment was $g = 0.024$ T/m. A spinning rate of 20 Hz was used in the experiments with sample spinning.

4. Results and discussion

4.1 SLIC

Fig. 2 compares the singlet relaxation decays obtained from a sample of 1-(ethyl-d_5) 4-(propyl- d_7) (*Z*)-but-2-enedioate using a SLIC singlet excitation technique [12] on both a 500 MHz and a 600 MHz spectrometers with and without sample spinning. In the pulse sequence shown in Figure 2A, the initial 90˚ pulse converts equilibrium longitudinal spin order into transverse magnetization (triplet coherence). Then, a spin-lock induced crossing (SLIC) pulse is applied along the x-magnetization for coherent transfer of the magnetization into singlet order. The singlet state is then stored undisturbed during the singlet relaxation period followed by the ZQ filtration sequence. During the ZQ filtration, three sine-bell shaped gradients of various amplitudes along with the rf pulses effectively suppress the single- and double-quantum coherences to prevent their undesirable interference with the detected signal [44]. After that, the second SLIC pulse is used to convert singlet spin order into single-quantum coherence (transverse magnetization) that is immediately detected. It can be seen that the curves obtained without spinning show significantly faster decay rates than the spinning samples. Furthermore, the experiment at 600 MHz shows an oscillatory behavior, presumably arising from convective circulation of the fluid similar to the one observed previously in T_1 inversion-recovery experiments [36]. Sample spinning, however, increases the apparent singlet lifetime and

eliminates the decay distortions which indicates that convection is suppressed significantly. As was discussed above, convection losses occur when molecules bearing singlet order leave the region where the singlet is effectively generated and detected. As a result, part of the singlet order can never be detected and is thus lost. The experiments recorded on a cryoprobe show more drastic effects (Fig. 2B, 600 MHz), most likely due to the larger temperature gradients that are generated from the presence of the low-temperature tuned circuit. The experimental curve for a nonspinning sample in a cryoprobe was fit using the convection model described by Eq. 2 in order to determine whether the experimental features could be reproduced with reasonable parameters. The Rayleigh number for this simulation was 1400 which for chloroform corresponded to a temperature gradient of 1.65 K/cm. As seen in Fig. 2, a good agreement between simulated (dashed) and experimental curves is found, which indicates the adequacy of the model in spite of the significant limiting assumptions.

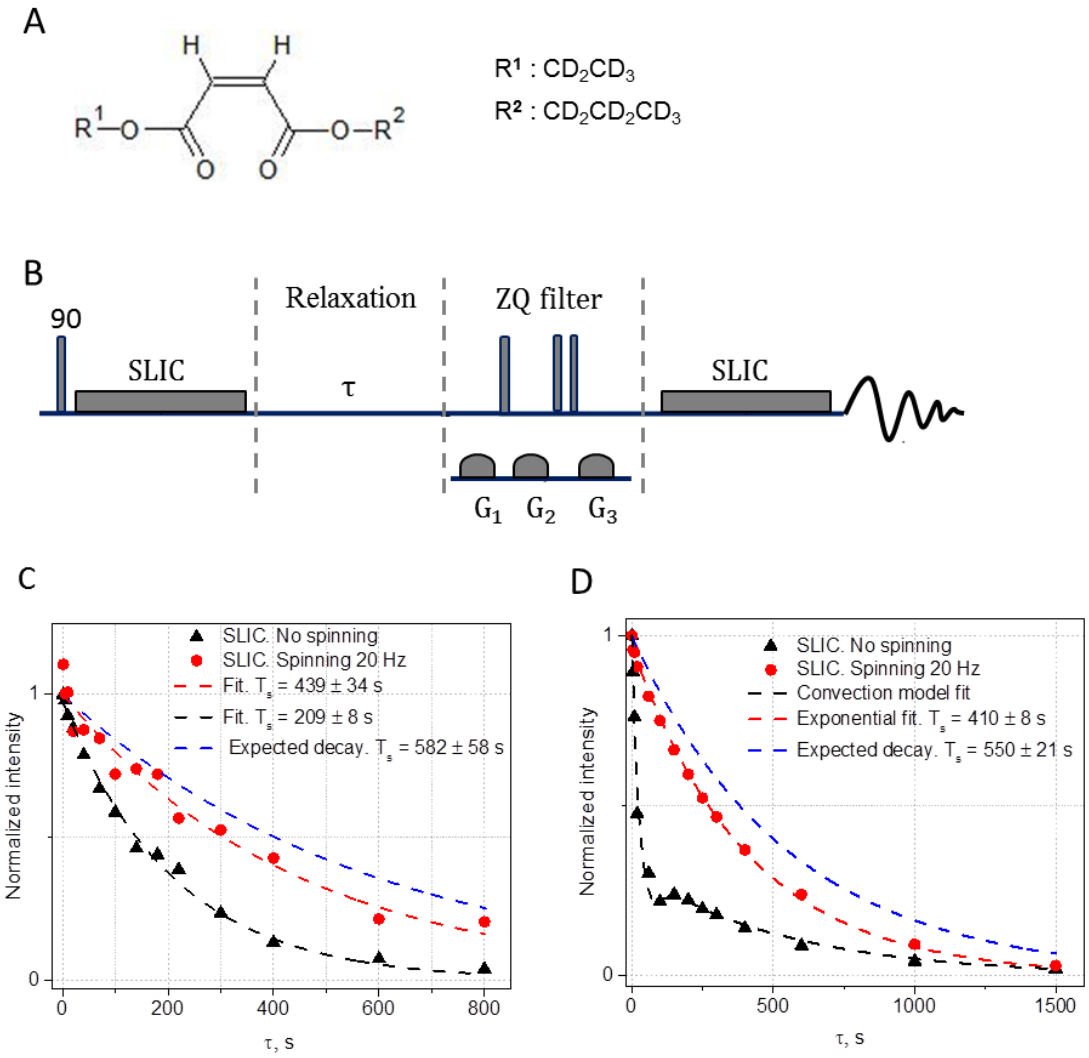

Fig. 2. (A) The 1-(ethyl-d_5) 4-(propyl- d_7) (*Z*)-but-2-enedioate molecule. (B) SLIC pulse sequence in (C) a 500 MHz spectrometer with a room temperature probe, and (D), a 600 MHz spectrometer equipped with a cryoprobe.

Figure 3 shows the comparison of ^{1}H 1D-images obtained using the same pulse sequence, together with a readout gradient, which allows one to map the excitation profiles over the sample volume. As can be seen in Figure 3, singlet excitation is greatly inhomogeneous even in the coil region. It can be seen that singlet order is efficiently created and reconverted to detectably magnetization mainly at the edges of the coil. In fact, molecular displacement even within the coil region thus leads to signal loss. We have examined whether simply rescaling the rf power of the SLIC would significantly change the excitation/detection patterns, and make it more uniform, but this was not the case. This finding points to the fact that the observed effects are not solely caused by B_1 inhomogeneity.

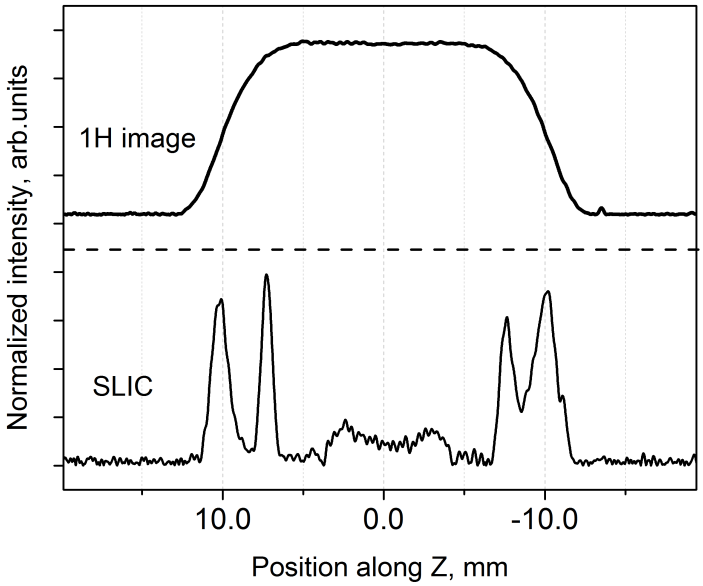

Fig. 3. Comparison of 1D z-images obtained using the SLIC singlet excitation (bottom) and back-conversion method and a conventional ^{1}H image (top) obtained from the DMM solution.

To avoid molecules leaving the coil region, one can use shorter or confined samples but this procedure has certain practical disadvantages. For example, susceptibility-matched plugs are available only for a few solvents, and the use of these plugs is very difficult to combine with the requirement of efficient sample degassing, which is often needed for the measurement of true singlet lifetimes. If susceptibility-matched plugs are not used, significant line broadening may be observed. Broad-band SLIC modifications exist [14, 45] and demonstrate high effectiveness, but these techniques often cannot overcome the concomitant broadening. For ^{1}H singlet applications, the applied spin-lock field power must match the intra-singlet J-coupling, and the bandwidth of applied spin-lock pulses, even for the best demonstrated adiabatic SLIC versions is of the order of B_1 amplitude, 10-20 Hz. On the other hand, the spectral width of a short sample is typically significantly broader than that, which makes it impossible to uniformly excite the entire spectral

line using a spin-lock based triplet-singlet conversion technique. Nonetheless, adiabatic SLIC [14] is potentially applicable for heteronuclei. For example, in ^{13}C singlet spectroscopy, the in-pair J-coupling and hence the spin-lock power are often much larger than the line width.

4.2 M2S with composite inversion pulses

To avoid complications associated with line broadening when short samples are used, broadband singlet excitation methods, such as M2S (Fig. 2A), need to be employed. The M2S sequence has the advantage of being broad-band with respect to resonance offsets, and thus may offer the first step in improving the situation. Furthermore, inhomogeneities due to susceptibility differences in a short sample would not affect the results much. M2S has no long narrow-band elements and is not sensitive to offset effects. Therefore, the spectral width has no effect on the singlet conversion efficiency. Moreover, one can use composite universal rotation pulses in J-coupling synchronized pulse trains in M2S. This approach increases the robustness of the pulse sequence to B_1 mismatches. It is advantageous to use composite pulses for the repeating π-rotation elements, thus eliminating or minimizing an accumulation of errors. Non-repeating elements of these sequences are not so critical, since they do not cause significant errors.

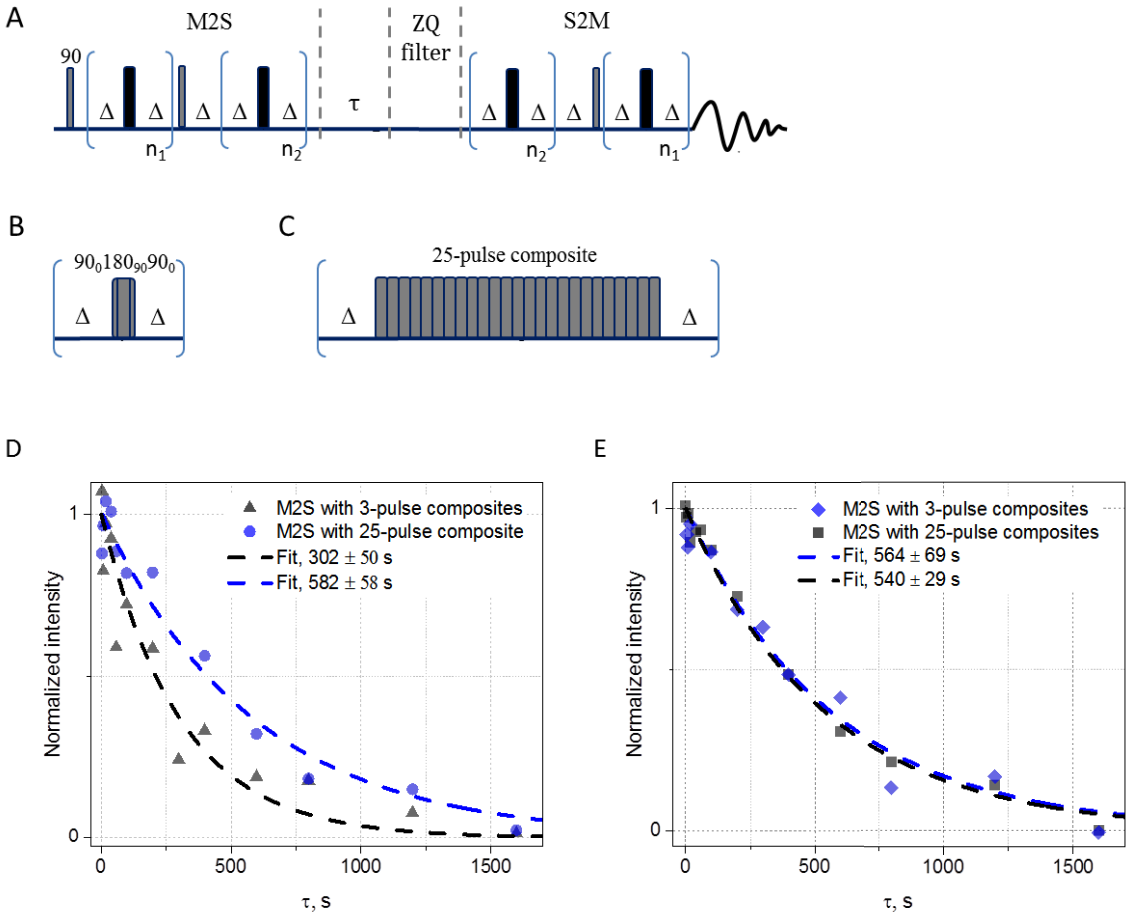

Fig. 4. (A) M2S pulse sequence; composite pulses are shown as black rectangles. Two composite inversion elements used in this work: (B) $90_0180_{90}90_0$ and (C) the 25 pulse composite, that consists of twenty-five 180˚ pulses

[46, 47] (phases indicated in the text). Comparison of singlet relaxation decays obtained in a short sample of a solution of the compound of Fig. 2A using M2S with 3- and 25-pulse composite inversion pulses without (D) and with sample spinning (E).

Figure 4 (D, E) compares the singlet relaxation curves obtained using M2S with different composite inversion elements with and without sample spinning, respectively. The first one is the widely-used 90-180-90 composite pulse applied with the MLEV4 phase incremental scheme [43]. It is compared to an M2S sequence with every 180º pulse is replaced by a highly B_1 mismatch-compensated pulse train consisting of twenty-five 180-pulses with phases 0, 0, 120, 60, 120, 0, 0, 120, 60, 120, 120, 120, 240, 180, 240, 60, 60, 180, 120, 180, 120, 120, 240, 180, 240 [46, 47]. It can be seen that the apparent singlet lifetime increased by a factor of almost two when the highly compensated composites were used. The experiments with sample spinning demonstrate similar results for both types of composite pulses in the M2S sequence, while they agree best with the result from the 25-pulse sequence without spinning. These results illustrate that a B1 inhomogeneity must be a significant factor in the observed signal losses.

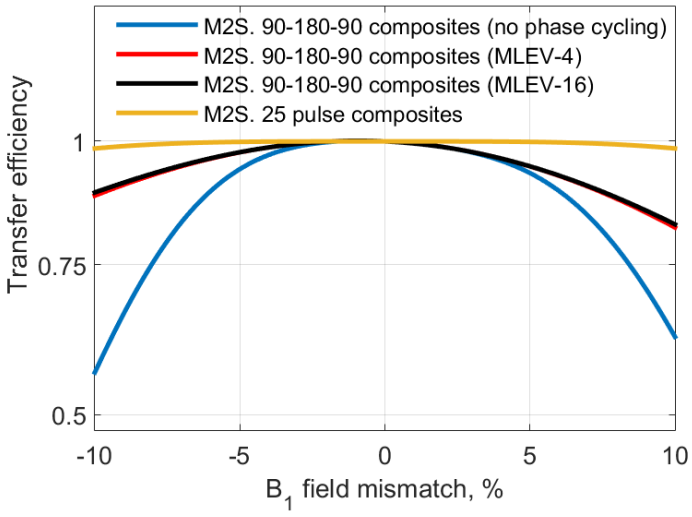

Fig. 5. Dependence of simulated normalized singlet transfer efficiency in a M2S experiment for the parameters of a the compound of Fig. 2A (J = 12 Hz, $\Delta\nu$ = 1 Hz) vs. B_1-field mismatch. Composite universal rotation pulses are compared.

Figure 5 illustrates the dependence of the normalized transfer efficiency in a full M2S experiment on B_1 field mismatch. The simulation shows that the singlet excitation/detection efficiency significantly depends on the B_1 field homogeneity for the sequence with 3-pulse composites with and without phase cycling. An implementation with phase cycling provides higher transfer efficiency and flatter B_1 mismatch dependence than when no phase cycle was used. The comparison of two phase incremental schemes, MLEV4 [43] and MLEV16 [48], shows no significant difference in transfer efficiency. On the other hand, the 25-pulse composite inversion element provides a highly uniform excitation in the entire B_1 inhomogeneity range of a

typical NMR probe. Phase cycling for this composite pulse has no significant effect on the transfer efficiency.

The 25-pulse composite provides the highest-possible performance over the whole sample volume when the sample is located entirely within the active coil region, which eliminates possible loss of signal as a result of convection. In this implementation, we were thus able to measure the longest singlet lifetimes for this sample – 582 s. We note that B_1 inhomogeneity alone could not explain these results, but sample motion in combination with these inhomogeneities appears to be the underlying mechanism, and efficient compensation of these inhomogeneities provides a method for measuring lifetimes in a robust way.

5. Conclusions

We have shown that a reduction of the measured singlet relaxation rates is due to the interplay between two processes: macroscopic motion in the sample and non-uniformity of singlet excitation and detection due to rf field inhomogeneity. The macroscopic motion, due to thermal convection currents, leads to a relocation of molecules between singlet creation and detection, and thus an additional time-dependent decay is seen in the experiments. In drastic situations, molecules can also leave the coil region, but even when the samples are confined, significant additional decays are observed. To overcome these problems, we demonstrate that control of convection enhances the ability to measure long singlet lifetimes, and broad-band singlet conversion pulse elements, such as M2S/S2M, in combination with high-order composite pulse elements in M2S provide significant improvements in inhomogeneity compensation, and convection robustness. With these modifications, reliable singlet lifetime measurements may be obtained.

Acknowledgements

This work was supported by NSF grants CHE-1412568 (J.C.), CHE-0957586 (A.J.), and a joint grant CHE-1412064. The experiments were performed in the Shared Instrument Facility of the Department of Chemistry, New York University, supported by the US National Science Foundation under Grant No. CHE0116222. The Bruker Avance-500 NMR Spectrometer was acquired through the support of the National Science Foundation under Award Number CHE-01162222.

References

[1] M. Carravetta, M.H. Levitt, Long-Lived Nuclear Spin States in High-Field Solution NMR, J Am Chem Soc, 126 (2004) 6228-6229.

[2] M. Carravetta, O.G. Johannessen, M.H. Levitt, Beyond the ${T}_{1}$ Limit: Singlet Nuclear Spin States in Low Magnetic Fields, Phys Rev Lett, 92 (2004) 153003.
[3] M. Carravetta, M.H. Levitt, Theory of long-lived nuclear spin states in solution nuclear magnetic resonance. I. Singlet states in low magnetic field, J Chem Phys, 122 (2005).
[4] E. Vinogradov, A.K. Grant, Long-lived states in solution NMR: Selection rules for intramolecular dipolar relaxation in low magnetic fields, J Magn Reson, 188 (2007) 176-182.
[5] A.K. Grant, E. Vinogradov, Long-lived states in solution NMR: Theoretical examples in three- and four-spin systems, J Magn Reson, 193 (2008) 177-190.
[6] W.S. Warren, E. Jenista, R.T. Branca, X. Chen, Increasing Hyperpolarized Spin Lifetimes Through True Singlet Eigenstates, Science, 323 (2009) 1711-1714.
[7] G. Pileio, M.H. Levitt, Theory of long-lived nuclear spin states in solution nuclear magnetic resonance. II. Singlet spin locking, J Chem Phys, 130 (2009).
[8] G. Pileio, J.T. Hill-Cousins, S. Mitchell, I. Kuprov, L.J. Brown, R.C.D. Brown, M.H. Levitt, Long-Lived Nuclear Singlet Order in Near-Equivalent 13C Spin Pairs, J Am Chem Soc, 134 (2012) 17494-17497.
[9] M.H. Levitt, Symmetry constraints on spin dynamics: Application to hyperpolarized NMR, J Magn Reson, 262 (2016) 91-99.
[10] G. Pileio, M. Carravetta, E. Hughes, M.H. Levitt, The Long-Lived Nuclear Singlet State of 15N-Nitrous Oxide in Solution, J Am Chem Soc, 130 (2008) 12582-12583.
[11] G. Stevanato, J.T. Hill-Cousins, P. Håkansson, S.S. Roy, L.J. Brown, R.C.D. Brown, G. Pileio, M.H. Levitt, A Nuclear Singlet Lifetime of More than One Hour in Room-Temperature Solution, Angewandte Chemie International Edition, 54 (2015) 3740-3743.
[12] S.J. DeVience, R.L. Walsworth, M.S. Rosen, Preparation of Nuclear Spin Singlet States Using Spin-Lock Induced Crossing, Phys Rev Lett, 111 (2013).
[13] Y. Feng, T. Theis, T.L. Wu, K. Claytor, W.S. Warren, Long-lived polarization protected by symmetry, J Chem Phys, 141 (2014).
[14] T. Theis, Y. Feng, T. Wu, W.S. Warren, Composite and shaped pulses for efficient and robust pumping of disconnected eigenstates in magnetic resonance, J Chem Phys, 140 (2014).
[15] Y. Zhang, K. Basu, J.W. Canary, A. Jerschow, Singlet lifetime measurements in an all-proton chemically equivalent spin system by hyperpolarization and weak spin lock transfers, Phys Chem Chem Phys, 17 (2015) 24370-24375.
[16] Y. Zhang, X. Duan, P.C. Soon, V. Sychrovský, J.W. Canary, A. Jerschow, Limits in Proton Nuclear Singlet-State Lifetimes Measured with para-Hydrogen-Induced Polarization, Chemphyschem, 17 (2016) 2967-2971.
[17] G. Pileio, M. Carravetta, M.H. Levitt, Storage of nuclear magnetization as long-lived singlet order in low magnetic field, P Natl Acad Sci USA, 107 (2010) 17135-17139.
[18] M.C.D. Tayler, M.H. Levitt, Singlet nuclear magnetic resonance of nearly-equivalent spins, Phys Chem Chem Phys, 13 (2011) 5556-5560.
[19] M.H. Levitt, Singlet Nuclear Magnetic Resonance, Annual Review of Physical Chemistry, Vol 63, 63 (2012) 89-105.
[20] D. Graafen, M.B. Franzoni, L.M. Schreiber, H.W. Spiess, K. Munnemann, Magnetic resonance imaging of H-1 long lived states derived from parahydrogen induced polarization in a clinical system, J Magn Reson, 262 (2016) 68-72.
[21] J.N. Dumez, J.T. Hill-Cousins, R.C.D. Brown, G. Pileio, Long-lived localization in magnetic resonance imaging, J Magn Reson, 246 (2014) 27-30.
[22] S. Cavadini, J. Dittmer, S. Antonijevic, G. Bodenhausen, Slow Diffusion by Singlet State NMR Spectroscopy, J Am Chem Soc, 127 (2005) 15744-15748.
[23] R. Sarkar, P.R. Vasos, G. Bodenhausen, Singlet-State Exchange NMR Spectroscopy for the Study of Very Slow Dynamic Processes, J Am Chem Soc, 129 (2007) 328-334.
[24] P. Ahuja, R. Sarkar, P.R. Vasos, G. Bodenhausen, Diffusion Coefficients of Biomolecules Using Long-Lived Spin States, J Am Chem Soc, 131 (2009) 7498-7499.

[25] G. Pileio, J.N. Dumez, I.A. Pop, J.T. Hill-Cousins, R.C.D. Brown, Real-space imaging of macroscopic diffusion and slow flow by singlet tagging MRI, J Magn Reson, 252 (2015) 130-134.
[26] P. Ahuja, R. Sarkar, P.R. Vasos, G. Bodenhausen, Molecular properties determined from the relaxation of long-lived spin states, J Chem Phys, 127 (2007).
[27] M.C.D. Tayler, S. Marie, A. Ganesan, M.H. Levitt, Determination of Molecular Torsion Angles Using Nuclear Singlet Relaxation, J Am Chem Soc, 132 (2010) 8225-8227.
[28] N. Salvi, R. Buratto, A. Bornet, S. Ulzega, I. Rentero Rebollo, A. Angelini, C. Heinis, G. Bodenhausen, Boosting the Sensitivity of Ligand–Protein Screening by NMR of Long-Lived States, J Am Chem Soc, 134 (2012) 11076-11079.
[29] P.R. Vasos, A. Comment, R. Sarkar, P. Ahuja, S. Jannin, J.-P. Ansermet, J.A. Konter, P. Hautle, B. van den Brandt, G. Bodenhausen, Long-lived states to sustain hyperpolarized magnetization, Proceedings of the National Academy of Sciences, 106 (2009) 18469-18473.
[30] G. Pileio, Relaxation theory of nuclear singlet states in two spin-1/2 systems, Prog Nucl Mag Res Sp, 56 (2010) 217-231.
[31] J.A. Aguilar, R.W. Adams, M. Nilsson, G.A. Morris, Suppressing exchange effects in diffusion-ordered NMR spectroscopy, J Magn Reson, 238 (2014) 16-19.
[32] A. Jerschow, N. Muller, Suppression of convection artifacts in stimulated-echo diffusion experiments. Double-stimulated-echo experiments, J Magn Reson, 125 (1997) 372-375.
[33] G. Zheng, W.S. Price, Simultaneous convection compensation and solvent suppression in biomolecular NMR diffusion experiments, J Biomol Nmr, 45 (2009) 295.
[34] K.I. Momot, P.W. Kuchel, Convection-compensating PGSE experiment incorporating excitation-sculpting water suppression (CONVEX), J Magn Reson, 169 (2004) 92-101.
[35] A. Jerschow, N. Müller, Convection compensation in gradient enhanced nuclear magnetic resonance spectroscopy, Journal of Magnetic Resonance, 132 (1998) 13-18.
[36] J. Lounila, K. Oikarinen, P. Ingman, J. Jokisaari, Effects of thermal convection on NMR and their elimination by sample rotation, J Magn Reson Ser A, 118 (1996) 50-54.
[37] H.Y. Chen, Y. Lee, S. Bowen, C. Hilty, Spontaneous emission of NMR signals in hyperpolarized proton spin systems, J Magn Reson, 208 (2011) 204-209.
[38] N.M. Loening, J. Keeler, Temperature accuracy and temperature gradients in solution-state NMR spectrometers, J Magn Reson, 159 (2002) 55-61.
[39] G.A. Ostroumov, Free convection under the conditions of the internal problem, National Advisory Committee for Aeronautics, Technical Memorandum 1407 (1958).
[40] A. Jerschow, Thermal convection currents in NMR: Flow profiles and implications for coherence pathway selection, J Magn Reson, 145 (2000) 125-131.
[41] I. Swan, M. Reid, P.W.A. Howe, M.A. Connell, M. Nilsson, M.A. Moore, G.A. Morris, Sample convection in liquid-state NMR: Why it is always with us, and what we can do about it, J Magn Reson, 252 (2015) 120-129.
[42] G. Stevanato, S.S. Roy, J. Hill-Cousins, I. Kuprov, L.J. Brown, R.C.D. Brown, G. Pileio, M.H. Levitt, Long-lived nuclear spin states far from magnetic equivalence, Phys Chem Chem Phys, 17 (2015) 5913-5922.
[43] M.H. Levitt, R. Freeman, Composite pulse decoupling, Journal of Magnetic Resonance (1969), 43 (1981) 502-507.
[44] M.C.D. Tayler, M.H. Levitt, Accessing Long-Lived Nuclear Spin Order by Isotope-Induced Symmetry Breaking, J Am Chem Soc, 135 (2013) 2120-2123.
[45] A.N. Pravdivtsev, A.S. Kiryutin, A.V. Yurkovskaya, H.-M. Vieth, K.L. Ivanov, Robust conversion of singlet spin order in coupled spin-1/2 pairs by adiabatically ramped RF-fields, J Magn Reson, 273 (2016) 56-64.
[46] M.H. Levitt, Composite Pulses, Prog Nucl Mag Res Sp, 18 (1986) 61-122.
[47] R. Tycko, A. Pines, Iterative schemes for broad-band and narrow-band population inversion in NMR, Chem Phys Lett, 111 (1984) 462-467.

[48] R. Freeman, T. Frenkiel, M.H. Levitt, A simple “black-box” decoupler, Journal of Magnetic Resonance (1969), 50 (1982) 345-348.